Defence Research and Development Canada
Recherche et développement pour la défense Canada

DRDC | RDDC

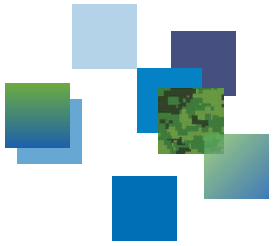

Analysis of matched filter mismatch for focusing moving targets in multi-channel synthetic aperture radar

David Kirkland
DRDC – Ottawa Research Centre

Defence Research and Development Canada

Scientific Report
DRDC-RDDC-2014-R51
September 2014

Canada

Analysis of matched filter mismatch for focusing moving targets in multi-channel synthetic aperture radar

David Kirkland
DRDC – Ottawa Research Centre

Defence Research and Development Canada
Scientific Report
DRDC-RDDC-2014-R51
September 2014

Abstract

This report derives the matched filter necessary for focusing moving targets in multi-channel Synthetic Aperture Radar (SAR) systems after clutter cancellation has been performed. The Displaced Phase Centre Antenna (DPCA) is utilized to achieve the clutter cancellation in a two channel SAR system. After deriving the matched filter, the tolerance of the filter is then analyzed for mismatches against errors in the moving target's position and velocity components. The tolerances are quantified for two exemplar SAR systems; an X-band airborne SAR and a C-band satellite SAR. The analysis also reveals when simplified versions of the matched filter can be used.

Significance for defence and security

The ability to generate a focused image of a moving target buried in stationary clutter can provide increased intelligence and can improve the performance of automatic target recognition (ATR) algorithms. Moving Target Indication (MTI) techniques are often focused at detecting slow moving targets. In SAR images these slow moving targets are fairly well-focused, although they may be displaced in the image from their true location. The use of Space-Time Adaptive Processing (STAP) techniques in combination with SAR imaging has been discussed in the literature already. However, the exact nature of the resulting moving target signature and how to produce a focused image of the moving target has not been extensively studied. This report is aimed addressing this shortcoming. Additionally, the parameters extracted from focusing the moving target can utilized in tracking algorithms.

This report derives the moving target's velocity tolerances necessary to produce a focused image of the moving target. These velocity tolerances are calculated for a typical airborne X-band SAR system and for a satellite C-band SAR system with parameters similar to RADARSAT-2.

Résumé

Le présent rapport indique les calculs relatifs au filtre adapté nécessaire pour focaliser des objectifs mobiles dans les systèmes radar à synthèse d'ouverture (SAR) multicanaux après avoir éliminé les échos parasites (clutter). L'antenne à centre de phase déplacé (DPCA) est utilisée pour éliminer le clutter dans un système SAR à deux canaux. Une fois que les caractéristiques du filtre adapté sont calculées, la tolérance de ce filtre est analysée pour trouver les défauts d'adaptation par rapport aux erreurs dans les composantes de position et de vitesse de l'objectif mobile. La tolérance est calculée pour deux systèmes SAR de référence : un SAR aéroporté en bande X et un SAR satellitaire en bande C. L'analyse montre aussi à quel moment on peut utiliser des versions simplifiées du filtre adapté.

Importance pour la défense et la sécurité

La capacité de produire une image focalisée d'un objectif mobile caché dans du clutter stationnaire peut fournir des renseignements supplémentaires et améliorer les performances des algorithmes de reconnaissance automatique des objectifs (ATR). Les techniques de visualisation des cibles mobiles (VCM) visent souvent à détecter des objectifs mobiles lents. Dans les images SAR, ces objectifs mobiles lents sont assez bien focalisés, même s'ils sont parfois déplacés dans l'image par rapport à leur position réelle. L'utilisation conjointe des techniques de traitement spatio-temporel adaptatif (STAP) et de l'imagerie SAR a déjà fait l'objet d'études . Par contre, la nature exacte de la signature résultante d'un objectif mobile et la production d'une image focalisée de l'objectif mobile n'ont pas été étudiées à fond. Le présent rapport vise à corriger cette lacune. De plus, les paramètres extraits de la focalisation de l'objectif mobile peuvent être utilisés dans les algorithmes de poursuite.

Le présent rapport indique les calculs relatifs aux tolérances de vitesse d'un objectif mobile qui sont nécessaires pour produire une image focalisée de cet objectif. Ces tolérances de vitesse sont calculées pour un système SAR aéroporté type en bande X et un système SAR satellitaire en bande C ayant des paramètres similaires à ceux de RADARSAT 2.

Table of contents

List of figures

1 Introduction

The effect of a moving target in Synthetic Aperture Radar (SAR) imagery was first analyzed in [1]. Subsequently, algorithms were developed to focus the moving target within the SAR image for single channel systems [2, 3, 4, 5]. Unfortunately, it is not possible to simultaneously focus the moving target and the stationary background in a single channel system. Additionally, it is often only possible to focus the moving target response when the stationary background clutter is relatively weak in comparison with the moving target, since the motion parameters necessary for focusing the moving target have to be estimated.

Ground Moving Target Indication (GMTI) systems utilize multiple channels to effectively cancel out the stationary clutter and detect a moving target [6]. A key metric of interest for GMTI applications is the minimum detectable velocity (MDV). Faster moving targets are usually easier to detect due to the increased Doppler separation between the moving target signal and the stationary background clutter [7]. SAR processing for stationary targets will produce a fairly well-focused SAR image for slow moving targets. In terms of focusing moving targets, the main interest lies in the higher velocity targets, which produce smearing and range migration effects in the resulting uncompensated SAR imagery [1].

This report conducts a theoretical analysis of the use of a multi-channel SAR system in a Displaced Phase Centre Antenna (DPCA) configuration to allow the focusing of the moving target signature when it is buried in the stationary clutter. Section 1.2 develops the signal model for the Spotlight SAR model. The Spotlight SAR configuration is used since it allows the formation of higher resolution imagery in comparison to Stripmap imagery operating with the same parameters. Section 1.3 describes the DPCA imaging geometry. Section 1.4 describes the signal models for the stationary clutter, the moving target signature and the resulting signal after DPCA clutter suppression. Section 2 examines the output of the matched filter and the sensitivities to the mismatch of the moving target motion parameters.

1.1 Mathematical notation

In this report we deal with signals in both temporal and spatial dimensions. For a temporal signal, the variables t and ω denote time and its Fourier counterpart temporal frequency respectively. The units of t and ω are seconds and radians/second respectively. The temporal Fourier transform of a signal $s(t)$ is denoted as $S(\omega)$,

where:

$$\begin{aligned} S(\omega) &= \mathcal{F}_t[s(t)] \\ &= \int_{-\infty}^{\infty} s(t) \exp(-j\omega t)\, d\, t. \end{aligned} \tag{1}$$

The inverse temporal Fourier transform of a signal $S(\omega)$ is identified as:

$$\begin{aligned} s(t) &= F_{\omega}^{-1}\left[S(\omega)\right] \\ &= \frac{1}{2\pi} \int_{-\infty}^{\infty} S(\omega) \exp(j\omega t)\, d\, \omega. \end{aligned} \tag{2}$$

For convenience, we define the wavenumber, k, as:

$$k = \frac{\omega}{c}, \tag{3}$$

where c is the speed of light. The unit of k is radians/meter.

For signals in the spatial domain u, the Fourier counterpart is spatial frequency k_u, which is also called the wavenumber. The units of u and k_u are meters and radians per meter respectively. The forward Fourier transform of a spatial domain signal $g(u)$ is denoted as $G(k_u)$, where:

$$\begin{aligned} G(k_u) &= \mathcal{F}_u[g(u)] \\ &= \int_{-\infty}^{\infty} g(u) \exp(-jk_u u)\, d\, u. \end{aligned} \tag{4}$$

The inverse spatial Fourier transform of a signal $G(k_u)$ is identified as:

$$\begin{aligned} g(u) &= F_{k_u}^{-1}\left[G(k_u)\right] \\ &= \frac{1}{2\pi} \int_{-\infty}^{\infty} G(k_u) \exp(jk_u u)\, d\, k_u. \end{aligned} \tag{5}$$

For convenience, we will use the symbol $\rightleftharpoons$ to denote a Fourier transform pair, that is:

$$s(t) \rightleftharpoons S(\omega), \tag{6}$$

$$g(u) \rightleftharpoons G(k_u). \tag{7}$$

1.2 Signal model

The data collection geometry for the radar is shown in Figure 1. The instantaneous radar position is given by $(0, u)$, where u denotes the position of the radar platform in the cross-range direction. X_c and Y_c denote the centre of the spotlight scene in the range and cross-range directions respectively. The instantaneous position of a moving target is given by $(X_c + x_0 + v_x u, Y_c + y_0 + v_y u)$, where x_0 and y_0 denote the initial offset position of the moving target from the scene centre in the range and cross-range directions respectively. v_x and v_y denote the moving target's velocities in the range and cross-range directions respectively. For convenience the velocity components of the moving target have been normalized by the radar platform velocity.

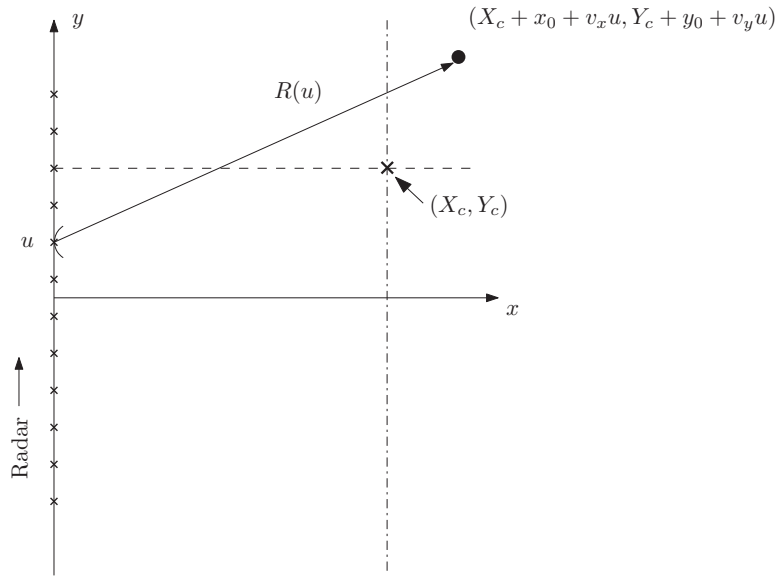

Figure 1: *SAR Imaging Geometry.*

After range compression, basebanding and motion compensation to a point, the received radar signal for the moving target, $S(\omega, u)$, in the frequency/cross-range domain can be written as:

$$S(\omega, u) = P(\omega) \exp\left(j\phi(\omega, u)\right), \tag{8}$$

where:

$$\phi(\omega, u) = -2(k + k_0)R_\Delta(u), \tag{9}$$

$$R_\Delta(u) = R(u) - R_{ref}(u), \tag{10}$$

$$R(u) = \sqrt{(X_c + x_0 + v_x u)^2 + (Y_c + y_0 + v_y u - u)^2}, \tag{11}$$

$$R_{ref}(u) = \sqrt{(X_c)^2 + (Y_c - u)^2}, \tag{12}$$

where $P(\omega)$ denotes the Fourier transform of the pulse compressed envelope, k_0 is the wavenumber corresponding to the radar centre frequency f_0, c is the speed of light, $k = \frac{\omega}{c}$ is the fast-time wavenumber (relative to k_0), and $\phi(\omega, u)$ denotes the phase response of the moving target. $R_{ref}(u)$ is the reference range, and corresponds to the instantaneous distance between the radar platform and the imaging scene centre. In the subsequent section dealing with DPCA, each channel will have a response similar to that shown in (8) but each channel will have an unique instantaneous range $R(u)$ and reference range $R_{ref}(u)$.

This development of the signal model has neglected to include the antenna beam pattern. The impact of the antenna beam pattern on the signal model developed in (8), is to introduce an amplitude modulation in the cross-range direction. For the purpose of image formation we are mostly interested in the phase portion of the response and therefore the antenna pattern has been omitted from (8) and from the subsequent analysis. In order for a DPCA system to achieve clutter cancellation the two-way beam patterns for the Transmit/Receive pairs must be identical. When the beam patterns are not identical then channel balancing procedure is required to achieve effective cancellation.

1.3 DPCA imaging geometry

The Displaced Phase Centre Array (DPCA) geometry typically involves a single transmitter and two receivers. The DPCA condition implies that the array moves a specific distance between consecutive pulses such that adjacent pulses at the two receivers can be subtracted to remove the stationary clutter.

In this report a modified array geometry is utilized to ease the burden of the mathematical analysis that follows which examines the sensitivity to the mismatch of focusing parameters. In this geometry we assume that there are two transmitter/receiver pairs denoted as Tx_1, Rx_1, Tx_2, Rx_2. Tx_1 and Rx_1 are collocated and Tx_2 and Rx_2 are collocated. Tx_1 and Tx_2 are separated by a distance d. The SAR system is assumed to move the distance d between consecutive pulses i.e., meets the DPCA condition. This geometry is illustrated in Figure 2.

The position of Tx_1/Rx_1 is given by $(0, u)$, and the position of Tx_2/Rx_2 is given by $(0, u-d)$. The instantaneous range between Tx_1/Rx_1 and the stationary target point $(X_c + x_0, Y_c + y_0)$ is denoted as $R_1(u)$ and is given by:

$$R_1(u) = \sqrt{(X_c + x_0) + (Y_c + y_0 - u)^2}. \tag{13}$$

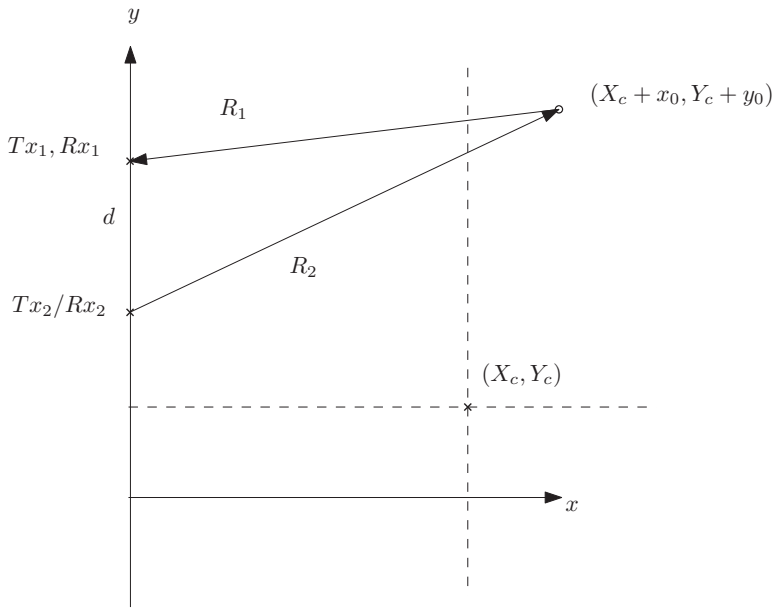

Figure 2: *DPCA Geometry.*

Similarly, the instantaneous range between Tx_2/Rx_2 and target point (X_c+x_0, Y_c+y_0) is denoted as $R_2(u)$ and is given by:

$$R_2(u) = \sqrt{(X_c + x_0)^2 + (Y_c + y_0 - u + d)^2}. \tag{14}$$

It is straightforward to see that $R_1(u-d) = R_2(u)$, and therefore the DPCA condition is met when the inter-pulse distance is equal to d.

1.4 Moving target

We now develop the range equations for a moving target. Consider a target with velocities v_x and v_y in the range and cross-range directions respectively. As before, the velocities have been normalized by the radar platform velocity. If the initial position of the target is $(X_c + x_0, Y_c + y_0)$, then instantaneous position of the moving target is given by $(X_c + x_0 + v_x u, Y_c + y_0 + v_y u)$ and the instantaneous range between Tx_1/Rx_1 and moving target is given by:

$$R_1(u) = \sqrt{(X_c + x_0 + v_x u)^2 + (Y_c + y_0 + v_y u - u)^2}. \tag{15}$$

Similarly, the instantaneous range between Tx_2/Rx_2 and moving target is given by:

$$R_2(u) = \sqrt{(X_c + x_0 + v_x u)^2 + (Y_c + y_0 + v_y u - u + d)^2}. \tag{16}$$

For convenience we define two reference ranges. These reference ranges are used in the motion compensation to a point procedure necessary for Spotlight image formation.

The reference range $R_{ref1}(u)$ denotes the distance between the Tx_1 and the scene centre (X_c, Y_c), and is given by:

$$R_{ref1}(u) = \sqrt{(X_c)^2 + (Y_c - u)^2}. \tag{17}$$

The second reference range, $R_{ref2}(u)$ denotes the distance between the Tx_2 and the scene centre (X_c, Y_c), and is given by:

$$R_{ref2}(u) = \sqrt{(X_c)^2 + (Y_c - u + d)^2}. \tag{18}$$

Again it is straightforward to verify that $R_{ref1}(u - d) = R_{ref2}(u)$.

In general the received signal after range compression in the fast-time frequency / cross-range domain is denoted by $S_{rx}(k, u)$, where:

$$S_{rx}(k, u) = P(\omega) \exp(-j2(k + k_0)R(u)), \tag{19}$$

where k is the fast-time wavenumber, $k_0 = 2\pi f_0/c$ is the wavenumber corresponding to the radar centre frequency f_0, $P(\omega)$ is the pulse compression response. After performing the motion compensation to a point, the resulting signal, $S(k, u)$ is given by:

$$S(k, u) = P(\omega) \exp(-j2(k + k_0)(R(u) - R_{ref}(u))), \tag{20}$$

where $R_{ref}(u)$ is the instantaneous distance from the platform to the scene centre.

The signal $S_1(k, u)$ from the Tx_1/Rx_1 pair is then given by:

$$\begin{aligned} S_1(k, u) &= P(\omega) \exp(-j2(k + k_0)(R_1(u) - R_{ref1}(u))) \\ &= P(\omega) \exp(-j2(k + k_0)\Delta R_1(u)), \end{aligned} \tag{21}$$

where $\Delta R_1(u) = R_1(u) - R_{ref1}(u)$. Similarly, the signal $S_2(k, u)$ from the Tx_2/Rx_2 pair is then given by:

$$\begin{aligned} S_2(k, u) &= P(\omega) \exp(-j2(k + k_0)(R_2(u) - R_{ref2}(u))) \\ &= P(\omega) \exp(-j2(k + k_0)\Delta R_2(u)), \end{aligned} \tag{22}$$

where $\Delta R_2(u) = R_2(u) - R_{ref2}(u)$. It should be noted that the removal of the reference ranges, $R_{ref1}(u)$ and $R_{ref2}(u)$, in this manner essentially applies a deramping function in the cross-range dimension of the data. The result of this deramping procedure is that the reference point or scene center is focused. This procedure is often referred to as motion compensation to a point and is often used in the Polar Format imaging algorithm for Spotlight SAR imaging [8, 9].

The result of the DPCA cancellation, $S_c(k,u)$ is given by:

$$\begin{aligned} S_c(k,u) &= S_1(k,u-d) - S_2(k,u) \\ &= P(\omega)\left[\exp(-j2(k+k_0)\Delta R_1(u-d)) - \exp(-j(k+k_0)\Delta R_2(u))\right]. \end{aligned} \tag{23}$$

From the previous properties of the range equations it can be seen that the stationary targets will be removed from the signal $S_c(k,u)$, while the moving targets will remain. Expanding $\Delta R_1(u)$, and $\Delta R_2(u)$ in a Taylor series w.r.t. the variables x_0, y_0, v_x, v_y about the point $x_0 = y_0 = v_x = v_y = 0$ gives (see [4]):

$$\Delta R_1(u) \approx \frac{X_c(x_0 + v_x u)}{R_{ref1}(u)} + \frac{(Y_c - u)(y_0 + v_y u)}{R_{ref1}(u)}, \tag{24}$$

$$\begin{aligned} \Delta R_2(u) &\approx \frac{X_c(x_0 + v_x u)}{R_{ref2}(u)} + \frac{(Y_c - u + d)(y_0 + v_y u)}{R_{ref2}(u)} \\ &= \cos\theta_2(u)(x_0 + v_x u) + \sin\theta_2(u)(y_0 + v_y u), \end{aligned} \tag{25}$$

where:

$$\cos\theta_2(u) = \frac{X_c}{R_{ref2}(u)}, \tag{26}$$

and

$$\sin\theta_2(u) = \frac{(Y_c - u + d)}{R_{ref2}(u)}. \tag{27}$$

It should be noted that:

$$R_{ref1}(u-d) = R_{ref2}(u), \tag{28}$$

and

$$\begin{aligned} \Delta R_1(u-d) &= \frac{X_c(x_0 + v_x(u-d))}{R_{ref2}(u)} + \frac{(Y_c - u + d)(y_0 + v_y(u-d))}{R_{ref2}(u)} \\ &= \cos\theta_2(u)(x_0 + v_x u - v_x d) + \sin\theta_2(u)(y_0 + v_y u - v_y d). \end{aligned} \tag{29}$$

It has been shown previously how squint Spotlight mode operation can be treated as a rotated geometry of the broadside Spotlight mode [4, 5, 10]. For convenience we then examine the broadside case where $\theta_2(0) = 0$, without any loss of generality. In Appendix A the following Taylor series approximations are developed:

$$\cos\theta_2(u) \approx 1 + \frac{d}{X_c^2}u - \frac{u^2}{2X_c^2},$$

and

$$\sin\theta_2(u) \approx \frac{d}{X_c} - \frac{u}{X_c}.$$

Applying these approximations to (25) and (29) gives:

$$\begin{aligned}\Delta R_1(u-d) &= \left(1 + \frac{d}{X_c^2}u - \frac{u^2}{2X_c^2}\right)(x_0 + v_x u - v_x d) + \left(\frac{d}{X_c} - \frac{u}{X_c}\right)(y_0 + v_y u - v_y d) \\ &= x_0 + \frac{d}{X_c}y_0 - dv_x - \frac{d^2}{X_c}v_y + \left(v_x + \frac{dx_0}{X_c^2} - \frac{d^2 v_x}{X_c^2} - \frac{y_0}{X_c} + \frac{2dv_y}{X_c}\right)u \\ &\quad + \left(\frac{3dv_x - x_0}{2X_c^2} - \frac{v_y}{X_c}\right)u^2 - \frac{v_x}{2X_c^2}u^3,\end{aligned} \tag{30}$$

and

$$\begin{aligned}\Delta R_2(u) &= \left(1 + \frac{d}{X_c^2}u - \frac{u^2}{2X_c^2}\right)(x_0 + v_x u) + \left(\frac{d}{X_c} - \frac{u}{X_c}\right)(y_0 + v_y u) \\ &= x_0 + \frac{d}{X_c}y_0 + \left(v_x + \frac{dx_0}{X_c^2} - \frac{y_0}{X_c} + \frac{dv_y}{X_c}\right)u + \left(\frac{2dv_x - x_0}{2X_c^2} - \frac{v_y}{X_c}\right)u^2 - \frac{v_x}{2X_c^2}u^3,\end{aligned} \tag{31}$$

Examination of the components of $\Delta R_1(u-d)$, and $\Delta R_2(u)$ reveals that they are quite similar in structure, but the presence of the moving target introduces some additional terms. In fact, it is these terms which enables DPCA and Space Time Adaptive Processing (STAP) techniques to detect moving targets in clutter. There is a constant difference of $-v_x d - \frac{d^2}{X_c}v_y$ between $\Delta R_1(u-d)$ and $\Delta R_2(u)$. The dominate component of this offset will usually be the $-v_x d$ term, since $d \ll X_c$. The linear components of $\Delta R_1(u-d)$ and $\Delta R_2(u)$ differ by the term $-\frac{v_y d}{X_c}u$. An extra term, given by $\frac{v_x d}{2X_c^2}$, appears in the quadratic component of $\Delta R_1(u-d)$. The cubic terms of $\Delta R_1(u-d)$ and $\Delta R_2(u)$ are identical.

In deriving these equations a flat-earth model has been used to simply the nature of the calculations. For an airborne geometry this assumption is usually adequate. For spaceborne SAR geometries additional adjustments are required to accommodate the curvature of the Earth and the gravitational force the Earth contributes to the equations of motion of the SAR platform. In [11, 12] it is shown that for a single channel system the SAR equations need only a slight modification by defining an "effective" satellite velocity. The SAR equations for a Multi-Channel Stripmap mode geometry are developed in [13]. In the analysis of this report the reference range from the satellite antennas to a stationary point on the Earth is removed from the signal model (see (21) and (22)). The reference ranges are exact i.e., no approximation has been made - however, in the satellite case the reference ranges will no longer be of the

form given in (17) and (18). The result of removing these reference ranges is the the reference point is focused in the SAR signal. This is the first processing step in the Polar format algorithm for Spotlight mode imaging. Therefore, the resulting Taylor series which are developed for ΔR_1 and ΔR_2 will still be applicable for the satellite geometry.

2 Matched filter analysis

In section 1.4 we developed the expression for the moving target signal after the cancellation of the stationary clutter. To form a focused image of the moving target a matched filter needs to be applied to the resulting moving target signature. Section 2.1 develops the necessary matched filter and derives the range of parameters over which the output of the matched filter can be expected to produce focused targets. Section 2.2 analyzes the output of the matched filter when the filter is mismatched to the moving target's motion parameters.

2.1 DPCA matched filter

After DPCA cancellation, a focused image of the moving target can be formed by applying a matched filter to (23). In some sense, this is similar to time domain matched filter processing. It forms an image of desired point and assumes an invariance region around that point i.e the centre point is focused but points further away suffer from some defocusing. An alternative, is to use Polar format processing and apply the matched filter afterwards.

Based on the output of the stationary clutter cancellation in (23) the matched filter $M(k,u)$ for focusing a moving target is given by:

$$\begin{aligned} M(k,u) &= S_c^*(k,u) \\ &= \exp(j2(k+k_0)\Delta R_1(u-d)) - \exp(j2(k+k_0)\Delta R_2(u)). \end{aligned} \tag{32}$$

It should be noted that the $P(\omega)$ factor of the signal is not included in (32) since it is assumed that pulse compression has already been performed. The result of applying the matched filter to (23) is given by:

$$\begin{aligned} S_c(k,u)M(k,u) &= P(\omega)\left[\exp(j0) + \exp(j0) - \exp(-j2(k+k_0)(\Delta R_1(u-d) - \Delta R_2(u)))\right. \\ &\quad \left. - \exp(-j2(k+k_0)(\Delta R_2(u) - \Delta R_1(u-d)))\right] \\ &= P(\omega)\left[2 - \exp(-j2(k+k_0)(\Delta R_1(u-d) - \Delta R_2(u)))\right. \\ &\quad \left. - \exp(j2(k+k_0)(\Delta R_1(u-d) - \Delta R_2(u)))\right] \\ &= P(\omega)\left[2 - 2\cos(2(k+k_0)(\Delta R_1(u-d) - \Delta R_2(u)))\right]. \end{aligned} \tag{33}$$

In broadside mode the expression for $\Delta R_1(u-d) - \Delta R_2(u)$ simplifies to:

$$\begin{aligned}\Delta R_1(u-d) - \Delta R_2(u) &= x_0 + \frac{d}{X_c}y_0 - dv_x - \frac{d^2}{X_c}v_y + \left(v_x + \frac{dx_0}{X_c^2} - \frac{d^2 v_x}{X_c^2} - \frac{y_0}{X_c} + \frac{2dv_y}{X_c}\right)u \\ &\quad + \left(\frac{3dv_x - x_0}{2X_c^2} - \frac{v_y}{X_c}\right)u^2 - \frac{v_x}{2X_c^2}u^3 \\ &\quad - \left[x_0 + \frac{d}{X_c}y_0 + \left(v_x + \frac{dx_0}{X_c^2} - \frac{y_0}{X_c} + \frac{dv_y}{X_c}\right)u\right. \\ &\quad \left. - \left(\frac{x_0 - 2dv_x}{2X_c^2} + \frac{v_y}{X_c}\right)u^2 - \frac{v_x}{2X_c^2}u^3\right] \\ &= -dv_x - \frac{d^2}{X_c}v_y + \left(\frac{dv_y}{X_c} - \frac{d^2 v_x}{X_c^2}\right)u + \frac{v_x d}{2X_c^2}u^2 \\ &\approx -dv_x + \frac{dv_y}{X_c}u + \frac{v_x d}{2X_c^2}u^2,\end{aligned} \tag{34}$$

where it is assumed that $d \ll X_c$. Substituting (34) into (33) gives:

$$S_c(k,u)M(k,u) = P(\omega)\left[2 - 2\cos\left(2(k+k_0)\left(-dv_x + \frac{dv_y}{X_c}u + \frac{v_x d}{2X_c^2}u^2\right)\right)\right]. \tag{35}$$

A focused image of the moving target can then by obtained by taking the two dimensional Inverse Fourier transform of (35). The $2P(\omega)$ term in (35) is the baseline coherent gain of the matched filter. The cosine-based term will introduce spurious components into the SAR imagery which are dependent on the moving target's velocity parameters and the distance between the radar platforms i.e., d.

The $k_0 v_x d$ terms in the cosine portion of (35) will modulate the quiescent coherent gain i.e., it can add either constructively or destructively to the constant coherent gain provided by the first term of (35). The destructive interference leads to blind velocities and will be discussed further later on. It should be noted that the dominant portion of this term is due to the v_x velocity since d is usually much smaller than X_c. The $kv_x d$ terms in the cosine portion of (35) will result in duplicate targets appearing in the range direction in the resulting SAR imagery. The $(k+k_0)\frac{dv_y}{X_c}u$ term in the cosine portion of (35) results in range walk of the moving target and duplicate targets appearing in the cross-range dimension of the resulting SAR imagery. The $(k+k_0)\frac{dv_x}{X_c^2}u^2$ term in the cosine portion of (35) will produce range curvature and smearing in the cross-range dimension of the moving target in the corresponding SAR imagery.

An alternative viewpoint is to examine the effects of the target's velocity components on the output of the matched filter operation. The v_y velocity component of the

moving target will introduce duplicate targets in the cross-range and introduce range walk. The v_x velocity component of the moving target will introduce duplicate peaks in the range direction (due to the $v_x d$ term), cross-range smear and a range curvature component.

The output of the matched filter can be used to form a focused image of the moving target if the linear and quadratic components of the cosine term in (35) are limited. These limits will determine the maximum target velocities that can be imaged with the matched filter under the operating conditions of the radar platform i.e., aperture length, antenna separation, and operating frequency. The limits for the magnitudes of the target velocities can be established by limiting the range migration (range walk and range curvature) to be less than a range cell, limiting duplicate targets to be less than a resolution cell distance away (range and cross-range), and limiting quadratic phase errors to be less than $\pi/4$ [11, 8]. This results in the following five criteria:

1. To limit the range walk the shift should be less than one range cell at the extreme limit of the aperture i.e., u_{max}:

$$\begin{aligned} 2k_{max}\frac{|v_y|\,d}{X_c}u_{max} &< 2\pi \\ |v_y| &< \frac{\pi X_c}{u_{max}k_{max}d}. \end{aligned} \tag{36}$$

2. To limit the duplicate targets in the cross-range dimension the cross-range frequency component should be less than the cross-range resolution i.e., $2\pi/L$, where $L = u_{max} - u_{min}$. This results in the following constraint:

$$\begin{aligned} 2k_0\frac{|v_y d|}{X_c} &< \frac{2\pi}{L} \\ |v_y| &< \frac{\pi X_c}{Lk_0 d}. \end{aligned} \tag{37}$$

3. To limit the cross-range smear we limit the phase variation at the limit of the aperture i.e., u_{max}:

$$\begin{aligned} 2k_0\frac{|v_x|\,d}{2X_c^2}u_{max}^2 &< \frac{\pi}{4} \\ |v_x| &< \frac{\pi X_c^2}{k_0 d u_{max}^2}. \end{aligned} \tag{38}$$

4. To limit the range curvature the shift should be less than one range cell at the extreme limit of the aperture i.e., u_{max}:

$$\begin{aligned} 2k_{max}\frac{|v_x|\,d}{2X_c^2}u_{max}^2 &< 2\pi \\ |v_x| &< 2\pi\frac{X_c^2}{k_{max}du_{max}^2}. \end{aligned} \tag{39}$$

5. The limit the duplicate targets in the range direction we limit the shift to be less than one range cell, which produces the following constraint:

$$\begin{aligned} 2k_{max}\left|v_x\right| d &< 2\pi \\ \left|v_x\right| &< \frac{\pi}{k_{max} d}. \end{aligned} \tag{40}$$

It should be noted that all of these criterion are inversely proportional to the phase centre separation. Therefore a smaller phase centre separation increases the range of velocities over which the matched filter will focus the moving target.

A further restriction occurs if we consider the operation of the system in conditions where the previous five criterion are all met. In this case the terms dependent on u become negligible and (35) is then reduced to:

$$S_c(k,u)M(k,u) = P(\omega)\left[2 - 2\cos\left(2(k+k_0)\left(-v_x d\right)\right)\right]. \tag{41}$$

In this form it is straightforward to see that the DPCA approach is prone to blind speeds when:

$$v_x = N\frac{\pi}{dk_0}, \tag{42}$$

where N is an integer. At these velocities the output of the canceler is almost zero over the bandwidth of the radar.

To illustrate the expected maximum velocities for typical radar systems, we have considered an X-band airborne radar system and a C-band satellite radar system. The parameters for the airborne and satellite radar systems are given in Table 1 and Table 2 respectively. Note that the both the theoretical cross-range resolution and pulse bandwidth are kept constant for both systems. The pulse bandwidth of $k_0 = 4.1867$ rad/m corresponds to 200 MHz.

Table 1: *Airborne radar parameters.*

Parameter	Value
k_0	188.5 rad/m
k_{max}	4.1867 rad/m
d	1 m
u_{max}	511 m
L	1022 m
X_c	20,000 m

The calculated velocity tolerances for the airborne and satellite radar systems are shown in Table 3 and Table 4 respectively. It should also be noted that the satellite velocity is on the order 7100 m/s and therefore the aperture illumination time corresponds to $73796/7100 = 10.4$ seconds.

Table 2: *Satellite radar parameters.*

Parameter	Value
k_0	111 rad/m
k_{max}	4.1867 rad/m
d	7.5 m
u_{max}	36898 m
L	73796 m
X_c	850 km

Table 3: *Maximum velocity constraints for an airborne radar with the operating parameters given in Table 1. For the blind velocities, N denotes any integer. Velocities are normalized by the platform velocity.*

Term	Limit
Range Walk	$\|v_y\| < 29.37$
Cross-Range Duplicates	$\|v_y\| < 0.3262$
Range Curvature	$\|v_x\| < 2299$
Cross-Range Smear	$\|v_x\| < 25.53$
Range Duplicates	$\|v_x\| < 0.7536$
Blind Velocities	$v_x = N16.6 \times 10^{-3}$

Table 4: *Maximum velocity constraints for a satellite radar system with the operating parameters given in Table 2. For the blind velocities, N denotes any integer. Velocities are normalized by the platform velocity.*

Term	Limit
Range Walk	$\|v_y\| < 2.3$
Cross-Range Duplicates	$\|v_y\| < 0.0435$
Range Curvature	$\|v_x\| < 106.2$
Cross-Range Smear	$\|v_x\| < 2.0$
Range Duplicates	$\|v_x\| < 0.1$
Blind Velocities	$v_x = N3.77 \times 10^{-3}$

2.2 DPCA matched filter mismatch

The previous analysis shows the output of the matched filter when the filter is perfectly matched to the incoming data. In this section the output of the matched filter when there is an error in the parameters (x_0, y_0, v_x, v_y), is explored. First we examine the situation when the matched filter is misaligned by $x_0 + \Delta x$. The resulting output is then given by:

$$\begin{aligned}
S(k,u,x)M(k,u,x+\Delta x) &= \exp\left(j2(k+k_0)\left(\Delta x + \frac{d\Delta x}{X_c^2}u - \frac{\Delta x}{2X_c^2}u^2\right)\right) \\
&+ \exp\left(j2(k+k_0)\left(\Delta x + \frac{d\Delta x}{X_c^2}u - \frac{\Delta x}{2X_c^2}u^2\right)\right) \\
&- \exp\left(j2(k+k_0)\left(\Delta x + v_x d + \frac{d\Delta x}{X_c^2}u - \frac{v_y d}{X_c}u - \frac{v_x d}{2X_c^2}u^2 - \frac{\Delta x}{2X_c^2}u^2\right)\right) \\
&- \exp\left(j2(k+k_0)\left(\Delta x - v_x d + \frac{d\Delta x}{X_c^2}u + \frac{v_y d}{X_c}u + \frac{v_x d}{2X_c^2}u^2 - \frac{\Delta x}{2X_c^2}u^2\right)\right) \qquad (43) \\
&= 2\exp\left(j2(k+k_0)\left(\Delta x + \frac{d\Delta x}{X_c^2}u - \frac{\Delta x}{2X_c^2}u^2\right)\right) \\
&- \exp\left(j2(k+k_0)\left(\Delta x + v_x d + \frac{d\Delta x}{X_c^2}u - \frac{v_y d}{X_c}u - \frac{v_x d}{2X_c^2}u^2 - \frac{\Delta x}{2X_c^2}u^2\right)\right) \\
&- \exp\left(j2(k+k_0)\left(\Delta x - v_x d + \frac{d\Delta x}{X_c^2}u + \frac{v_y d}{X_c}u + \frac{v_x d}{2X_c^2}u^2 - \frac{\Delta x}{2X_c^2}u^2\right)\right).
\end{aligned}$$

If we assume that the radar is operating under the five criteria listed in section 2.1 (see (36) - (40)) then the phase terms containing $\frac{v_y d}{X_c}u$ and $\frac{v_x d}{2X_c^2}u^2$ are insignificant and the following simplification is reached:

$$\begin{aligned}
S(k,u,x)M(k,u,x+\Delta x) \approx 2\exp&\left(j2(k+k_0)\left(\Delta x + \frac{d\Delta x}{X_c^2}u - \frac{\Delta x}{2X_c^2}u^2\right)\right) \\
&- \exp\left(j2(k+k_0)\left(\Delta x + v_x d + \frac{d\Delta x}{X_c^2}u - \frac{\Delta x}{2X_c^2}u^2\right)\right) \\
&- \exp\left(j2(k+k_0)\left(\Delta x - v_x d + \frac{d\Delta x}{X_c^2}u - \frac{\Delta x}{2X_c^2}u^2\right)\right). \qquad (44)
\end{aligned}$$

Examination of the phase elements of (44) reveals that the output of the matched filtering operation is shifted in the range direction by Δx, which is desirable for imaging purposes; however, the filter mismatch also introduces linear and quadratic terms, with respect to u, in the phase. The phase term $k\frac{d\Delta x}{X_c^2}u$ produces range walk in the resulting SAR image. To limit the range walk, the shift should be less than

one range cell at the limit of the aperture. This constraint produces the following inequality:

$$\begin{aligned} 2k_{max}\frac{d\,|\Delta x|}{X_c^2}u_{max} &< 2\pi \\ |\Delta x| &< \frac{\pi X_c^2}{dk_{max}u_{max}}. \end{aligned} \tag{45}$$

The other linear phase term, $k_0\frac{d\Delta x}{X_c^2}u$, produces a shift in the cross-range dimension of the SAR image. This does not affect the image formation process of the moving target.

The phase term $-j2(k+k_0)\frac{\Delta x}{2X_c^2}u^2$ introduces range curvature and a cross-range smear component in the resulting image. Limiting the effect of the range curvature to one resolution cell at the limit of the aperture requires:

$$\begin{aligned} 2k_{max}\frac{|\Delta x|}{2X_c^2}u_{max}^2 &< 2\pi \\ |\Delta x| &< \frac{2\pi X_c^2}{k_{max}u_{max}^2}. \end{aligned} \tag{46}$$

Limiting the cross-range smearing in the resulting imagery requires:

$$\begin{aligned} 2k_0\frac{|\Delta x|}{2X_c^2}u_{max}^2 &< \frac{\pi}{4} \\ |\Delta x| &< \frac{\pi X_c^2}{4k_0u_{max}^2}. \end{aligned} \tag{47}$$

Next we examine the situation when the filter is misaligned by $y_0 + \Delta y$. In this case the resulting output is given by:

$$\begin{aligned} S(k,u,x)M(k,u,y+\Delta y) = 2\exp&\left(j2(k+k_0)\left(\frac{d\Delta y}{X_c} - \frac{\Delta y}{X_c}u\right)\right) \\ &- \exp\left(j2(k+k_0)\left(v_xd + \frac{d\Delta y}{X_c} - \frac{\Delta y}{X_c}u - \frac{v_yd}{X_c}u - \frac{v_xd}{2X_c}u^2\right)\right) \\ &- \exp\left(j2(k+k_0)\left(-v_xd + \frac{d\Delta y}{X_c} - \frac{\Delta y}{X_c}u + \frac{v_yd}{X_c}u + \frac{v_xd}{2X_c^2}u^2\right)\right). \end{aligned} \tag{48}$$

Again, assuming that radar is operating such that the phase terms $\frac{v_yd}{X_c}u$ and $\frac{v_xd}{2X_c^2}u^2$are

insignificant produces the following:

$$\begin{aligned} S(k,u,x)M(k,u,y+\Delta y) \approx 2\exp\left(j2(k+k_0)\left(\frac{d\Delta y}{X_c}-\frac{\Delta y}{X_c}u\right)\right) \\ -\exp\left(j2(k+k_0)\left(v_x d+\frac{d\Delta y}{X_c}-\frac{\Delta y}{X_c}u\right)\right) \\ -\exp\left(j2(k+k_0)\left(-v_x d+\frac{d\Delta y}{X_c}-\frac{\Delta y}{X_c}u\right)\right). \end{aligned} \tag{49}$$

Examination of the phase of elements of (49) reveals the result of the mismatch produces not only an offset in the cross-range direction but also a range walk component. The offset in the cross-range dimension has no effect on the imaging results. However, limiting the range walk component to one range cell at the extreme of the aperture requires:

$$\begin{aligned} 2k_{max}\frac{|\Delta y|}{X_c}u_{max} &< 2\pi \\ |\Delta y| &< \frac{\pi X_c}{k_{max}u_{max}}. \end{aligned} \tag{50}$$

For the purpose of illustration the tolerances are calculated for the position mismatches (Δx, Δy) for the airborne and satellite radar systems analyzed in Section 2.1. Table 5 and Table 6 list the position mismatch constraints for the airborne and satellite radar geometry respectively. In both these geometries the tolerance for the range walk and the cross-range smear are the most dominant. For both these radar systems the matched filter would have to be recalculated every few resolution cells.

Table 5: *Position tolerances of matched filter for airborne radar with system parameters given in Table 1.*

Term	Limit
Range Walk	$\lvert\Delta x\rvert < 58.7$ km
Range Walk	$\lvert\Delta y\rvert < 29.37$ m
Range Curvature	$\lvert\Delta x\rvert < 2299$ m
Cross-Range Smear	$\lvert\Delta x\rvert < 6.38$ m

We examine the situation when the filter is mismatched by $v_x + \Delta v_x$. In this case the

Table 6: *Position tolerances of matched filter for satellite radar with system parameters given in Table 2.*

Term	Limit
Range Walk	$\lvert\Delta x\rvert < 1959$ km
Range Walk	$\lvert\Delta y\rvert < 17.28$ m
Range Curvature	$\lvert\Delta x\rvert < 796$ m
Cross-Range Smear	$\lvert\Delta x\rvert < 3.75$ m

output of the matched filter is given by:

$$\begin{aligned}
S(k,u,v_x)M(k,u,v_x+\Delta v_x) = &\exp\left(j2(k+k_0)\left(-d\Delta v_x+\Delta v_x u+\frac{3d\Delta v_x}{2X_c^2}u^2-\frac{\Delta v_x}{2X_c^2}u^3\right)\right)\\
&+\exp\left(j2(k+k_0)\left(\Delta v_x u+\frac{d\Delta v_x}{X_c^2}u^2-\frac{\Delta v_x}{2X_c^2}u^3\right)\right)\\
&-\exp\left(j2(k+k_0)\left(v_x d+\Delta v_x u-\frac{v_y d}{X_c}u+\frac{d\Delta v_x}{X_c^2}u^2\right.\right.\\
&\left.\left.-\frac{v_x d}{2X_c^2}u^2-\frac{\Delta v_x}{2X_c^2}u^3\right)\right)\\
&-\exp\left(j2(k+k_0)\left(-d\Delta v_x-v_x d+\Delta v_x u+\frac{v_y d}{X_c}u\right.\right.\\
&\left.\left.+\frac{3\Delta v_x d}{2X_c^2}u^2+\frac{v_x d}{2X_c^2}u^2-\frac{\Delta v_x}{2X_c^2}u^3\right)\right).
\end{aligned} \tag{51}$$

Again, assuming that the radar is operating such that the phase terms $\frac{v_y d}{X_c}u$ and $\frac{v_x d}{2X_c^2}u^2$ are insignificant produces the following:

$$\begin{aligned}
S(k,u,v_x)M(k,u,v_x+\Delta v_x) \approx &\exp\left(j2(k+k_0)\left(-d\Delta v_x+\Delta v_x u+\frac{3d\Delta v_x}{2X_c^2}u^2-\frac{\Delta v_x}{2X_c^2}u^3\right)\right)\\
&+\exp\left(j2(k+k_0)\left(\Delta v_x u+\frac{d\Delta v_x}{X_c^2}u^2-\frac{\Delta v_x}{2X_c^2}u^3\right)\right)\\
&-\exp\left(j2(k+k_0)\left(v_x d+\Delta v_x u+\frac{d\Delta v_x}{X_c^2}u^2-\frac{\Delta v_x}{2X_c^2}u^3\right)\right)\\
&-\exp\left(j2(k+k_0)\left(-d\Delta v_x-v_x d+\Delta v_x u+\frac{3\Delta v_x d}{2X_c^2}u^2\right.\right.\\
&\left.\left.+\frac{\Delta v_x d}{2X_c^2}u^2-\frac{\Delta v_x}{2X_c^2}u^3\right)\right).
\end{aligned} \tag{52}$$

As in the case for the position mismatch the velocity mismatch results in linear and quadratic phase errors; however an additional third order phase error emerges. The linear and quadratic phase errors will have the same effects as discussed previously. The third order phase error term introduces higher order range migration (third order) and produces asymmetrical sidelobes in the cross-range dimension of the SAR image [8].

Limiting the effect of duplicate targets in the range dimension to be less than one range cell apart requires:

$$\begin{aligned} 2k_{max}d\,|\Delta v_x| &< 2\pi \\ |\Delta v_x| &< \frac{\pi}{k_{max}d}. \end{aligned} \tag{53}$$

Limiting the range walk to be less than one range cell at the extreme limit of the aperture requires the following condition:

$$\begin{aligned} 2k_{max}\,|\Delta v_x|\,u_{max} &< 2\pi \\ |\Delta v_x| &< \frac{\pi}{k_{max}u_{max}}. \end{aligned} \tag{54}$$

Limiting the range curvature to be less than one range cell at the extreme limit of the aperture requires the following condition:

$$\begin{aligned} 2k_{max}\frac{|\Delta v_x|\,d}{2X_c^2}u_{max}^2 &< 2\pi \\ |\Delta v_x| &< \frac{2\pi X_c^2}{dk_{max}u_{max}^2}. \end{aligned} \tag{55}$$

In order to limit the cross-range smearing the maximum phase variation should be less than $\pi/4$ which requires:

$$\begin{aligned} 2k_0\frac{|\Delta v_x|\,d}{2X_c^2}u_{max}^2 &< \frac{\pi}{4} \\ |\Delta v_x| &< \frac{\pi X_c^2}{4dk_0u_{max}^2}. \end{aligned} \tag{56}$$

Imposing the same limit on the third order range migration to be less than one range resolution cell at the ends of the aperture produces the following condition:

$$\begin{aligned} 2k_{max}\frac{|\Delta v_x|}{2X_c^2}u_{max}^3 &< 2\pi \\ |\Delta v_x| &< \frac{2\pi X_c^2}{k_{max}u_{max}^3}. \end{aligned} \tag{57}$$

Limiting the phase error to be less than $\pi/4$ for the third order cross-range smearing term produces the following condition:

$$\begin{aligned} 2k_0 \frac{|\Delta v_x|}{2X_c^2} u_{max}^3 &< \frac{\pi}{4} \\ |\Delta v_x| &< \frac{\pi X_c^2}{k_0 u_{max}^3}. \end{aligned} \tag{58}$$

Table 7 and Table 8 list the constraints on Δv_x for the airborne geometry and the satellite geometry respectively. It is important to note that these velocities are given relative to the radar platform velocity. In both these geometries the limiting factor is driven by the range walk and third order cross-range smearing criterion. This increased sensitivity will result in a large number of matched filters for different v_x values for typical radar platform velocities and expected target motion velocities.

We examine the situation when the filter is mismatched by $v_y + \Delta v_y$. In this case the

Table 7: *Δv_x velocity tolerances for matched filter for airborne radar with system parameters given in Table 1.*

Term	Limit
Range Duplicate	$\lvert\Delta v_x\rvert < 0.75$
Range Walk	$\lvert\Delta v_x\rvert < 1.4 \times 10^{-3}$
Range Curvature	$\lvert\Delta v_x\rvert < 2298$
Cross-Range Smear	$\lvert\Delta v_x\rvert < 3261$
Third Order Range Migration	$\lvert\Delta v_x\rvert < 4.49$
Third Order Cross-Range Smear	$\lvert\Delta v_x\rvert < 49.9 \times 10^{-3}$

Table 8: *Δv_x velocity tolerances for matched filter for satellite radar with system parameters given in Table 2.*

Term	Limit
Range Duplicate	$\lvert\Delta v_x\rvert < 0.1$
Range Walk	$\lvert\Delta v_x\rvert < 2 \times 10^{-5}$
Range Curvature	$\lvert\Delta v_x\rvert < 106.2$
Cross-Range Smear	$\lvert\Delta v_x\rvert < 18472$
Third Order Range Migration	$\lvert\Delta v_x\rvert < 0.021$
Third Order Cross-Range Smear	$\lvert\Delta v_x\rvert < 4.0 \times 10^{-4}$

output of the matched filter is given by:

$$\begin{aligned} S(k,u,v_y)M(k,u,v_y+\Delta v_y) &= \exp\left(j2(k+k_0)\left(\frac{2d\Delta v_y}{X_c}u-\frac{\Delta v_y}{X_c}u^2\right)\right) \\ &+\exp\left(j2(k+k_0)\left(\frac{d\Delta v_y}{X_c}u-\frac{\Delta v_y}{X_c}u^2\right)\right) \\ &-\exp\left(j2(k+k_0)\left(v_x d+\frac{d\Delta v_y}{X_c}u-\frac{v_y d}{X_c}u-\frac{\Delta v_y}{X_c}u^2-\frac{v_x d}{2X_c^2}u^2\right)\right) \\ &-\exp\left(j2(k+k_0)\left(-v_x d+\frac{2d\Delta v_y}{X_c}u+\frac{v_y d}{X_c}u-\frac{\Delta v_y}{X_c}u^2+\frac{v_x d}{2X_c^2}u^2\right)\right). \end{aligned} \tag{59}$$

Again, assuming that the radar is operating under the conditions given by (36) - (40) then the phase terms $\frac{v_y d}{X_c}u$ and $\frac{v_x d}{2X_c^2}u^2$ are insignificant produces the following simplification:

$$\begin{aligned} S(k,u,v_y)M(k,u,v_y+\Delta v_y) &= \exp\left(j2(k+k_0)\left(\frac{2d\Delta v_y}{X_c}u-\frac{\Delta v_y}{X_c}u^2\right)\right) \\ &+\exp\left(j2(k+k_0)\left(\frac{d\Delta v_y}{X_c}u-\frac{\Delta v_y}{X_c}u^2\right)\right) \\ &-\exp\left(j2(k+k_0)\left(v_x d+\frac{d\Delta v_y}{X_c}u-\frac{\Delta v_y}{X_c}u^2\right)\right) \\ &-\exp\left(j2(k+k_0)\left(-v_x d+\frac{2d\Delta v_y}{X_c}u-\frac{\Delta v_y}{X_c}u^2\right)\right). \end{aligned} \tag{60}$$

Examination of the phase elements of (60) reveals the presence of undesirable linear and quadratic phase terms. The phase terms produce effects similar to those previously analyzed. Limiting the range walk to be less than one range cell at the extreme limit of the aperture produces following condition:

$$\begin{aligned} 2k_{max}\frac{|\Delta v_y|\,d}{X_c}u_{max} &< 2\pi \\ |\Delta v_y| &< \frac{\pi X_c}{dk_{max}u_{max}}. \end{aligned} \tag{61}$$

Limiting the range curvature to be less than one range cell at the extreme limit of the aperture, results in the following condition:

$$\begin{aligned} 2k_{max}\frac{|\Delta v_y|}{X_c^2}u_{max}^2 &< 2\pi \\ |\Delta v_y| &< \frac{\pi X_c^2}{k_{max}u_{max}^2}. \end{aligned} \tag{62}$$

Limiting the phase error to be less than $\pi/4$, in order to limit the cross-range smearing, requires the following condition:

$$\begin{aligned} 2k_0 \frac{|\Delta v_y|}{X_c^2} u_{max}^2 &< \frac{\pi}{4} \\ |\Delta v_y| &< \frac{\pi X_c^2}{8 k_0 u_{max}^2}. \end{aligned} \tag{63}$$

Table 9 and Table 10 list the constraints on Δv_y for the airborne and satellite radar geometries respectively . It is important to note that these velocities are given relative to the radar platform velocity. For both these geometries the most restrictive criterion is related to the range walk. However, for the typical radar platform velocities and expected range of target motion velocities these restrictions are not expected to be prohibitive. From the analysis of the tolerances for both position and velocity mismatches in the matched filter it is apparent that the dominating factors are the mismatches in both range and cross-range positions and the target's velocity in the range direction, i.e., v_x.

Table 9: *Δv_y velocity tolerances for matched filter for airborne radar with system parameters given in Table 1.*

Term	Limit
Range Walk	$\lvert\Delta v_y\rvert < 29.3$
Range Curvature	$\lvert\Delta v_y\rvert < 1149$
Cross-Range Smear	$\lvert\Delta v_y\rvert < 1630$

Table 10: *Δv_y velocity tolerances for matched filter for satellite radar with system parameters given in Table 2.*

Term	Limit
Range Walk	$\lvert\Delta v_y\rvert < 2.3$
Range Curvature	$\lvert\Delta v_y\rvert < 398$
Cross-Range Smear	$\lvert\Delta v_y\rvert < 69272$

3 Summary and conclusions

This report develops the matched filter necessary for focusing a moving target signature after DPCA processing. Due to the signal subtraction in the DPCA processing, the resulting imagery will contain artifacts. The appropriate limits on the range and cross-range velocities are derived to limit these artifacts and the corresponding values calculated for typical airborne and satellite geometries. In both these geometries the most stringent constraint is imposed by the limitation on the range and cross-range duplicates, which limit the range and cross-range velocity respectively of the target of interest.

Additionally, the effect of filter mismatch to the moving target's position and velocity has also been analyzed and the corresponding limits on the targets position and velocities used in the matched filter have been derived. For both the airborne and satellite geometries the limitation on cross-range smearing in the imagery imposes the tightest constraint on the range mismatch to the target. The mismatch in the target's range velocity is most tightly constrained by the range walk criterion for the both airborne and satellite geometries. However, the effect on third order cross-range smearing should also be examined. For both the airborne and satellite geometries the mismatch in the target's cross-range velocity is most tightly constrained by the limitation on range walk. However due to the relative insensitivity of the image formation process to cross-range velocity mismatch, this limitation is unlikely to pose any problems for most SAR systems.

This page intentionally left blank.

References

[1] Raney, R. K. (1971), Synthetic Aperture Imaging Radar and Moving Targets, *IEEE Transactions on Aerospace and Electronic Systems*, 7(3), 499–505.

[2] Perry, R., DiPietro, R., and Fante, R. (1999), SAR Imaging of Moving Targets, *IEEE Transactions on Aerospace and Electronic Systems*, 35(1), 188–200.

[3] Fienup, J. (2001), Detecting Moving Targets in SAR Imagery by Focusing, *IEEE Transactions on Aerospace and Electronic Systems*, 37(3), 794–808.

[4] Kirkland, D. (2011), Imaging Moving Targets Using the Second-Order Keystone Transform, *IET Radar Sonar and Navigation*, 5(8), 902–910.

[5] Kirkland, D. (2012), An Alternative Range Migration Correction Algorithm for Focusing Moving Targets, *Progress in Electromagnetics Research*, 131, 227–241.

[6] Klemm, R. (1998), Space-Time Adaptive Processing: Principles and Applications, The Institution of Electical Engineers.

[7] Richards, M. A. (2005), Fundamentals of Radar Signal Processing, First ed, McGraw Hill.

[8] Carrara, W., Goodman, R., and Majewski, R. (1995), Spotlight Synthetic Aperture Radar, Artech House.

[9] Soumekh, M. (1999), Synthetic Aperture Radar Signal Processing, First ed, John Wiley & Sons, Inc.

[10] Kirkland, D. (2013), Linear and Second Order Keystone Transforms and Their Applications, (Technical Report TM 2013-058) Defence R&D Canada - Ottawa.

[11] Curlander, J. C. and McDonough, R. N. (1991), Synthetic Aperture Radar Systems and Signal Processing, First ed, John Wiley & Sons, Inc.

[12] Cumming, I. and Wong, F. (2005), Digital Processing of Synthetic Aperture Radar Data, First ed, Artech House.

[13] Chiu, S. and Dragošević, M. (2009), Equations of motion of a ground moving target for a multi-channel spaceborne SAR, (Technical Report TM 2008-326) Defence R&D Canada - Ottawa.

This page intentionally left blank.

Annex A: Taylor series approximations for $\cos\theta_2$ and $\sin\theta_2$

In this section we derive the Taylor series formulas for $\cos\theta_2$ and $\sin\theta_2$. These are the most general cases. Other simpler cases can be found by setting the appropriate values to zero e.g., $Y_c = 0$. Further approximations can also be made by assuming $d = 0$, or $d \ll X_c$.

A.1 Approximation for $\cos\theta_2(u)$

From (26) the definition of $\cos\theta_2(u)$ is given as:

$$\cos\theta_2(u) = \frac{X_c}{\sqrt{{X_c}^2 + (Y_c - u + d)^2}}. \tag{A.1}$$

Evaluating $\cos\theta_2(u)$ at $u = 0$ gives:

$$\cos\theta_2(0) = \frac{X_c}{\sqrt{{X_c}^2 + (Y_c + d)^2}}. \tag{A.2}$$

Taking the first derivative of $\cos\theta_2(u)$ gives:

$$\begin{aligned} \frac{\partial \cos\theta_2(u)}{\partial u} &= -\frac{1}{2} X_c \left({X_c}^2 + (Y_c - u + d)^2\right)^{-\frac{3}{2}} (-2)(Y_c - u + d) \\ &= \frac{X_c(Y_c - u + d)}{({X_c}^2 + (Y_c - u + d)^2)^{\frac{3}{2}}}. \end{aligned} \tag{A.3}$$

Evaluating the first derivative at $u = 0$ gives:

$$\left.\frac{\partial \cos\theta_2(u)}{\partial u}\right|_{u=0} = \frac{X_c(Y_c + d)}{({X_c}^2 + (Y_c + d)^2)^{\frac{3}{2}}}. \tag{A.4}$$

Taking the second derivative of $\cos\theta_2(u)$ gives:

$$\begin{aligned} \frac{\partial^2 \cos\theta_2(u)}{\partial u^2} &= -\frac{X_c}{({X_c}^2 + (Y_c - u + d)^2)^{\frac{3}{2}}} - \frac{3}{2}\frac{X_c(Y_c - u + d)}{({X_c}^2 + (Y_c - u + d)^2)^{\frac{5}{2}}}(-2)(Y_c - u + d) \\ &= -\frac{X_c}{({X_c}^2 + (Y_c - u + d)^2)^{\frac{3}{2}}} + 3\frac{X_c(Y_c - u + d)^2}{({X_c}^2 + (Y_c - u + d)^2)^{\frac{5}{2}}}. \end{aligned} \tag{A.5}$$

Evaluating the second derivative at $u = 0$ gives:

$$\left.\frac{\partial^2 \cos\theta_2(u)}{\partial u^2}\right|_{u=0} = -\frac{X_c}{({X_c}^2 + (Y_c + d)^2)^{\frac{3}{2}}} + 3\frac{X_c(Y_c + d)^2}{({X_c}^2 + (Y_c + d)^2)^{\frac{5}{2}}}. \tag{A.6}$$

The Taylor series approximation for $\cos\theta_2(u)$ is then given as:

$$\begin{aligned}\cos\theta_2(u) \approx{}& \frac{X_c}{\sqrt{{X_c}^2 + (Y_c + d)^2}} + \frac{X_c(Y_c + d)}{({X_c}^2 + (Y_c + d)^2)^{\frac{3}{2}}}u \\ &+ \left[3\frac{X_c(Y_c + d)^2}{({X_c}^2 + (Y_c + d)^2)^{\frac{5}{2}}} - \frac{X_c}{({X_c}^2 + (Y_c + d)^2)^{\frac{3}{2}}}\right]\frac{u^2}{2}.\end{aligned} \tag{A.7}$$

For the broadside case, set $Y_c = 0$ which gives:

$$\begin{aligned}\cos\theta_2(u) &= \frac{X_c}{\sqrt{{X_c}^2 + d^2}} + \frac{X_c d}{({X_c}^2 + d^2)^{\frac{3}{2}}}u + \left(3\frac{X_c d^2}{({X_c}^2 + d^2)^{\frac{5}{2}}} - \frac{X_c}{({X_c}^2 + d^2)^{\frac{3}{2}}}\right)\frac{u^2}{2} \\ &\approx 1 + \frac{d}{X_c^2}u + \left(3\frac{d^2}{X_c^4} - \frac{1}{X_c^2}\right)\frac{u^2}{2}.\end{aligned} \tag{A.8}$$

In the case where $d \ll X_c$, and $0 \ll X_c$ then:

$$\cos\theta_2(u) \approx 1 + \frac{d}{X_c^2}u - \frac{u^2}{2X_c^2}. \tag{A.9}$$

In the particular case when $d = 0$ then:

$$\cos\theta(u) \approx 1 - \frac{u^2}{2X_c^2}. \tag{A.10}$$

A.2 Approximation for $\sin\theta_2(u)$

From (27) the definition of $\sin\theta_2(u)$ is given as:

$$\sin\theta_2(u) = \frac{Y_c - u + d}{\sqrt{{X_c}^2 + (Y_c - u + d)^2}}. \tag{A.11}$$

Evaluating $\sin\theta_2(u)$ at $u = 0$ gives:

$$\sin\theta_2(0) = \frac{Y_c + d}{\sqrt{{X_c}^2 + (Y_c + d)^2}}. \tag{A.12}$$

Taking the first derivative of $\sin\theta_2(u)$ gives:

$$\begin{aligned}\frac{\partial \sin\theta_2(u)}{\partial u} &= -\frac{1}{\sqrt{{X_c}^2+(Y_c-u+d)^2}} - \frac{1}{2}\frac{(Y_c-u+d)}{({X_c}^2+(Y_c-u+d)^2)^{\frac{3}{2}}}(-2)(Y_c-u+d) \\ &= -\frac{1}{({X_c}^2+(Y_c-u+d)^2)^{\frac{1}{2}}} + \frac{(Y_c-u+d)^2}{({X_c}^2+(Y_c-u+d)^2)^{\frac{3}{2}}}.\end{aligned} \tag{A.13}$$

Evaluating the first derivative at $u=0$ gives:

$$\left.\frac{\partial \sin\theta_2(u)}{\partial u}\right|_{u=0} = -\frac{1}{({X_c}^2+(Y_c+d)^2)^{\frac{1}{2}}} + \frac{(Y_c+d)^2}{({X_c}^2+(Y_c+d)^2)^{\frac{3}{2}}}. \tag{A.14}$$

The Taylor series approximation for $\sin\theta_2(u)$ is then given as:

$$\sin\theta_2(u) \approx \frac{Y_c+d}{\sqrt{{X_c}^2+(Y_c+d)^2}} + \left(\frac{(Y_c+d)^2}{({X_c}^2+(Y_c+d)^2)^{\frac{3}{2}}} - \frac{1}{({X_c}^2+(Y_c+d)^2)^{\frac{1}{2}}}\right)u. \tag{A.15}$$

For the broadside case, set $Y_c=0$ which gives:

$$\sin\theta_2(u) = \frac{d}{\sqrt{{X_c}^2+d^2}} + \left(\frac{d^2}{({X_c}^2+d^2)^{\frac{3}{2}}} - \frac{1}{({X_c}^2+d^2)^{\frac{1}{2}}}\right)u. \tag{A.16}$$

In the case where $d \ll X_c$, and $0 \ll X_c$ then:

$$\sin\theta_2(u) \approx \frac{d}{X_c} - \frac{u}{X_c}. \tag{A.17}$$

In the particular case when $d=0$ then:

$$\sin\theta(u) = -\frac{u}{X_c}. \tag{A.18}$$

This page intentionally left blank.

DOCUMENT CONTROL DATA

(Security markings for the title, abstract and indexing annotation must be entered when the document is Classified or Designated.)

1. ORIGINATOR (The name and address of the organization preparing the document. Organizations for whom the document was prepared, e.g. Centre sponsoring a contractor's report, or tasking agency, are entered in section 8.)

DRDC – Ottawa Research Centre
3701 Carling Avenue, Ottawa ON K1A 0Z4, Canada

2a. SECURITY MARKING (Overall security marking of the document, including supplemental markings if applicable.)

UNCLASSIFIED

2b. CONTROLLED GOODS

(NON-CONTROLLED GOODS)
DMC A
REVIEW: GCEC APRIL 2011

3. TITLE (The complete document title as indicated on the title page. Its classification should be indicated by the appropriate abbreviation (S, C or U) in parentheses after the title.)

Analysis of matched filter mismatch for focusing moving targets in multi-channel synthetic aperture radar

4. AUTHORS (Last name, followed by initials – ranks, titles, etc. not to be used.)

Kirkland, D.

5. DATE OF PUBLICATION (Month and year of publication of document.)	6a. NO. OF PAGES (Total containing information. Include Annexes, Appendices, etc.)	6b. NO. OF REFS (Total cited in document.)
September 2014	38	13

7. DESCRIPTIVE NOTES (The category of the document, e.g. technical report, technical note or memorandum. If appropriate, enter the type of report, e.g. interim, progress, summary, annual or final. Give the inclusive dates when a specific reporting period is covered.)

Scientific Report

8. SPONSORING ACTIVITY (The name of the department project office or laboratory sponsoring the research and development – include address.)

DRDC – Ottawa Research Centre
3701 Carling Avenue, Ottawa ON K1A 0Z4, Canada

9a. PROJECT OR GRANT NO. (If appropriate, the applicable research and development project or grant number under which the document was written. Please specify whether project or grant.)	9b. CONTRACT NO. (If appropriate, the applicable number under which the document was written.)
03mm	

10a. ORIGINATOR'S DOCUMENT NUMBER (The official document number by which the document is identified by the originating activity. This number must be unique to this document.)	10b. OTHER DOCUMENT NO(s). (Any other numbers which may be assigned this document either by the originator or by the sponsor.)
DRDC-RDDC-2014-R51	

11. DOCUMENT AVAILABILITY (Any limitations on further dissemination of the document, other than those imposed by security classification.)

(X) Unlimited distribution
( ) Defence departments and defence contractors; further distribution only as approved
( ) Defence departments and Canadian defence contractors; further distribution only as approved
( ) Government departments and agencies; further distribution only as approved
( ) Defence departments; further distribution only as approved
( ) Other (please specify):

12. DOCUMENT ANNOUNCEMENT (Any limitation to the bibliographic announcement of this document. This will normally correspond to the Document Availability (11). However, where further distribution (beyond the audience specified in (11)) is possible, a wider announcement audience may be selected.)

Unlimited

13. ABSTRACT (A brief and factual summary of the document. It may also appear elsewhere in the body of the document itself. It is highly desirable that the abstract of classified documents be unclassified. Each paragraph of the abstract shall begin with an indication of the security classification of the information in the paragraph (unless the document itself is unclassified) represented as (S), (C), or (U). It is not necessary to include here abstracts in both official languages unless the text is bilingual.)

This report derives the matched filter necessary for focusing moving targets in multi-channel Synthetic Aperture Radar (SAR) systems after clutter cancellation has been performed. The Displaced Phase Centre Antenna (DPCA) is utilized to achieve the clutter cancellation in a two channel SAR system. After deriving the matched filter, the tolerance of the filter is then analyzed for mismatches against errors in the moving target's position and velocity components. The tolerances are quantified for two exemplar SAR systems; an X-band airborne SAR and a C-band satellite SAR. The analysis also reveals when simplified versions of the matched filter can be used.

14. KEYWORDS, DESCRIPTORS or IDENTIFIERS (Technically meaningful terms or short phrases that characterize a document and could be helpful in cataloguing the document. They should be selected so that no security classification is required. Identifiers, such as equipment model designation, trade name, military project code name, geographic location may also be included. If possible keywords should be selected from a published thesaurus. e.g. Thesaurus of Engineering and Scientific Terms (TEST) and that thesaurus identified. If it is not possible to select indexing terms which are Unclassified, the classification of each should be indicated as with the title.)

SAR Imaging
DPCA
Moving Target Imaging
Multi-Channel

DRDC | RDDC

SCIENCE, TECHNOLOGY AND KNOWLEDGE FOR CANADA'S DEFENCE AND SECURITY | SCIENCE, TECHNOLOGIE ET SAVOIR POUR LA DÉFENSE ET LA SÉCURITÉ DU CANADA

www.drdc-rddc.gc.ca